

# Statistical properties of spectra in harmonically trapped spin-orbit coupled systems

O. V. Marchukov, A. G. Volosniev, D. V. Fedorov, A. S. Jensen, N. T. Zinner

*Department of Physics and Astronomy, Aarhus University, DK-8000 Aarhus C, Denmark*

(Dated: July 27, 2021)

We compute single-particle energy spectra for a one-body hamiltonian consisting of a two-dimensional deformed harmonic oscillator potential, the Rashba spin-orbit coupling and the Zeeman term. To investigate the statistical properties of the obtained spectra as functions of deformation, spin-orbit and Zeeman strengths we examine the distributions of the nearest neighbor spacings. We find that the shapes of these distributions depend strongly on the three potential parameters. We show that the obtained shapes in some cases can be well approximated with the standard Poisson, Brody and Wigner distributions. The Brody and Wigner distributions characterize irregular motion and help identify quantum chaotic systems. We present a special choices of deformation and spin-orbit strengths without the Zeeman term which provide a fair reproduction of the fourth-power repelling Wigner distribution. By adding the Zeeman field we can reproduce a Brody distribution, which is known to describe a transition between the Poisson and linear Wigner distributions.

## I. INTRODUCTION

Cold atomic gases are routinely trapped in spatially confining harmonic oscillator potentials [1–4]. The deformation of the trap gives us the opportunity to consider systems in lower dimensions. In this paper we discuss particles trapped in a two-dimensional (2D) harmonic trap which can be deformed (unequal trapping frequencies in transverse directions) and as a limiting case the one-dimensional (1D) harmonic trap. In addition, we put a spin-dependent one-body potential [5] that couples spin and motional degrees of freedom into a spin-orbit coupling. More specifically we discuss the famous spin-orbit term introduced by Rashba [6]. This type of spin-orbit coupling has not yet been realized with cold atomic gases, but there are recent proposals on how to proceed [7, 8].

In recent years other spin-orbit coupled systems were realized in state-of-the-art experiments for both bosonic [9–13] and fermionic systems [14, 15]. The case of spin-orbit coupled particles confined in a spherical harmonic oscillator trap have recently also drawn much attention from different groups [16–19]. In particular, large spin-orbit strengths are studied in the spherical trap where Landau-like levels then emerge. A more general anisotropic spin-orbit coupling in a 2D spherical trap has also been studied [20, 21]. Variation of the anisotropy changes the hamiltonian from Rashba to Dresselhaus coupling [22] which both result in identical spectra. In between one of the two spin-orbit terms has zero strength which implies a shifted 1D-oscillator spectrum with an offset of zero-point energy from the other direction. Thus, this variation is very similar to our variations where the spin-orbit is isotropic and the oscillator becomes strongly deformed. Sufficiently large deformation and isotropic spin-orbit is then similar to spherical oscillator and sufficiently large anisotropy of the spin-orbit coupling.

A two-dimensional spin-orbit coupled system has several interesting properties when tuning deformation, spin-orbit strength, and an additional Zeeman field. The resulting energy spectra exhibit large variations as func-

tion of the tunable external parameters [23]. Specifically, a given hamiltonian produces a density of states varying from extremely few to many states as function of energy. Under perturbations coming from interactions, low and high density of states can reflect stability and instability, respectively [24]. This can be related to the statistical properties of the single-particle eigenvalue spectrum.

In Ref. [23] a broad variety of spectra appeared depending on the controllable parameters of the external field. This means that the dynamical properties of the system can be flexibly and accurately tuned and investigated through appropriate analysis. Regular motion arising from integrable systems corresponds to a Poisson distribution for the nearest neighbor spacing (NNS). For the deformed harmonic oscillator this is not the case and the distribution depends on frequency ratios [25]. For irregular (chaotic) motion the eigenenergies avoid crossing appear between level separations. Then the celebrated Bohigas-Giannoni-Schmit conjecture [26] states that the statistical behavior of the levels can be described by random matrix theory. A semiclassical explanation can be found in Ref. [27].

The study of chaotic behaviour in cold atoms dates back at least two decades when it was suggested to use atoms in time-dependent optical lattices [28]. This proposal was realized shortly after by the Raizen group [29]. Later on the paradigmatic quantum delta-kicked rotor model found an experimental realization with atom optics [30] (see [31] for a more recent discussion of the experimental and theoretical investigations into this model). Experiments with large Cesium alkali atoms have also been performed [32, 33] and used to study localization and its relation to quantum chaotic phenomena. Common to most of these experiments is that the key quantity that is measured is the momentum distribution of the atoms by time-of-flight which is a well-established technique in cold atoms [1, 2]. The systems we consider in this paper can also be probed by mapping out the momentum distributions. Some more recent proposals to probe chaotic dynamics involve both cold atoms, molecules and ions [34–36], and just a few months ago atoms with large

magnetic dipole moments have shown experimental signs of chaotic behavior in their scattering dynamics [37].

The purpose of the present paper is to provide a statistical analysis of the energy spectrum arising from spin-orbit coupled non-interacting particles in a trap. We shall extract the properties covering regular as well as chaotic motion. More specifically we shall calculate the statistical distributions characterizing the spectra depending on the tunable parameters. This in turn points at the possible dynamical behavior. The paper is organized as follows: In Section II we first briefly give the connection between statistical properties and dynamical behavior. Then, after specifying the parameters of the system, we describe the adopted statistical treatment. Our numerical results are presented and discussed in Section III. Here we show the nearest neighbor spacing distribution for different values of trap deformation and spin-orbit coupling and Zeeman strengths. Finally, Section IV contains summary, conclusion and perspectives for future directions of research in this area.

## II. INGREDIENTS

Statistical analyses of spectra are meant to suggest which type of dynamical behavior is inherent to a given system. We therefore first elaborate on qualitative implications and possible distributions and their origin in connection with the present system. In the next subsections we specify hamiltonian, external parameters and describe the employed statistical procedure.

### A. Motivation and perspective

Dynamical evolution of a non-stationary state for a given hamiltonian is determined by the time dependent relative phases of the stationary states involved. Many unrelated energies quickly lead to loss of memory of an initial non-stationary state, and the Poincaré recurrence time becomes large tending to infinity when many states contribute. Future properties of the system becomes impossible to predict unless at least some average properties of the full spectrum is known. Vice versa, strongly related (for example equidistantly distributed) sets of energies lead to a regular oscillatory behavior, and predictions become entirely possible. These observations are directly relevant for one particle moving in an external one-body potential. The relevant energy range is then the width of the wave packet constituting the initial state.

For  $N$  non-interacting identical particles, where each is subject to the same one-body hamiltonian, the same spectrum is the basic ingredient. The relevant energy range is now obtained from the distribution of single-particle energies in the initial symmetric (bosons) or antisymmetric (fermions) many-body state. For fermions in their ground state the single-particle energy range is centered around the Fermi energy. When small uncer-

tainties are inherent in the external parameters we again encounter possible dynamical evolution of an initially defined wave packet of given energy and width. However, now these parameters are as well allowed to vary with time, presumably within rather restricted limits. We do not envisage this type of complicated dynamics, although our analyses and the results in this paper would have some bearing on these as well.

The dynamical behavior of a given system is necessarily contained in the quantum mechanical stationary solutions, and specifically in the energy spectrum. It is therefore of interest to investigate the statistical properties of the energy spectra as function of the parameters in the problem. In particular, the nearest neighbor spacing (NNS) distribution of energies carries information about the dynamical behavior [38]. The distributions emerging by following the statistical procedure can be compared to dimensionless standard distributions obtained from random matrix spectra with specified symmetries. We shall compare our results with the well known distributions named Poisson,  $P_P$ , and Wigner distributions where the latter appears in three variations,  $P_{W1}$ ,  $P_{W2}$  and  $P_{W4}$ . The variable,  $S > 0$ , is the energy difference between nearest neighbors in the energy spectrum. For numerical comparison we specify these normalized distributions, i.e.

$$P_P(S) = \exp(-S), \quad (1)$$

$$P_{W1}(S) = \frac{\pi S}{2} \exp\left(-\frac{\pi S^2}{4}\right), \quad (2)$$

$$P_{W2}(S) = \frac{32S^2}{\pi^2} \exp\left(-\frac{4S^2}{\pi}\right), \quad (3)$$

$$P_{W4}(S) = \frac{2^{18}S^4}{3^6\pi^3} \exp\left(-\frac{64S^2}{9\pi}\right). \quad (4)$$

A Poisson distribution is obtained for the nearest neighbor spacing for a random matrix spectrum when the system would exhibit classically regular motion or equivalently is integrable [39]. In quantum mechanics this corresponds to sufficiently many conserved quantum numbers. The energy levels are unaffected by the presence of its neighbors.

On the other hand, the three other distributions obtained from a random matrix spectrum corresponds to irregular motion where the levels do not cross. In this sense the levels repel each other and each energy level must keep some distance to its neighbors. This traditionally is the signature of quantum chaotic motion [39]. The three distributions are similar but with different powers  $\beta$  on  $S$  corresponding to different degrees of level repulsion. Indeed, when the neighboring energy levels come close together (i.e.  $S \rightarrow 0$ ) the distributions are defined by  $P(S) \sim S^\beta$ , where  $\beta = 1, 2, 4$ . Clearly an increasing  $\beta$  increases the size of the small  $S$  region of vanishing probability as seen in Fig. 1.

All the present statistical analyses are based on random matrix theory [40, 41], where matrix properties are analyzed under various assumptions of inherent symmetries. Antiunitarity, like time-reversal symmetry, re-

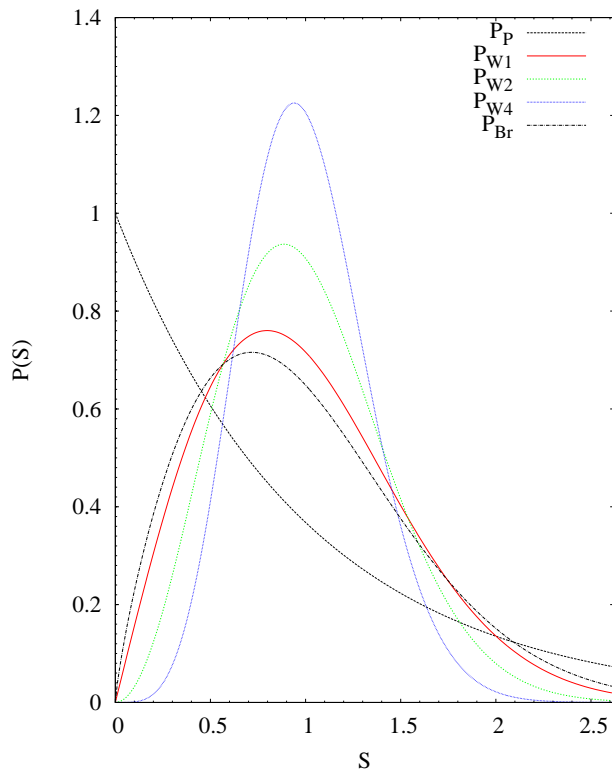


FIG. 1: The five standard distributions in Eqs.(1)-(5). Here  $P_P$  is peaked at small  $S$ , and the peaks for the three Wigner distributions move to larger  $S$ -values as the power of  $S$  increases. The Brody distribution is plotted for a value of the Brody parameter of  $\kappa = 0.4$

stricts the form of the hamiltonian and the corresponding matrix properties, and defines the power,  $\beta$ , of the level repulsion  $\beta$  [39]. There are three universal degrees of level repulsion: The  $\beta = 1$  case corresponds to the systems with integer spin and invariant under time-reversal and with some spatial rotational and/or reflection symmetry. The half-integer spin particles with time reversal symmetry and broken geometric symmetries correspond to  $\beta = 4$ . We have an interest in the latter symmetry because it corresponds to deformed systems with the Rashba spin-orbit interaction [39, 42]. If the time-reversal symmetry is broken by e.g. a magnetic field, then the system is described by  $\beta = 2$ .

The transition between the Poisson, Eq.(1), and linear Wigner, Eq.(2), distributions can be described by the so-called Brody distribution [43, 44], which is expressed as

$$P_{Br}(S) = (\kappa + 1)bS^\kappa \exp(-bS^{\kappa+1}), \quad (5)$$

where  $\kappa$  ( $0 \leq \kappa \leq 1$ ) is the Brody parameter and  $b = \left[ \Gamma\left(\frac{\kappa+2}{\kappa+1}\right) \right]^{\kappa+1}$ . It is shown in Fig. 1 for an intermediate  $\kappa$ -parameter, and it is straightforward to see the two limits of Poisson (1) and Wigner (2) distributions obtained for  $\kappa = 0$  and  $\kappa = 1$ , respectively. The physical meaning of the Brody parameter  $\kappa$  can be defined only

in particular cases [45].

## B. System specifications

We investigate a system of spin-orbit coupled non-interacting identical particles of mass  $m$  trapped in a harmonic potential. The spin-orbit coupling term depends only on  $x$ - and  $y$ -coordinates, and the motion in the  $z$ -direction can be easily decoupled. Hence, we will only consider the 2D hamiltonian. We also consider the Zeeman term which, for example, can appear by applying an external magnetic field. The one-body hamiltonian for the system is given by

$$\hat{H} = \left( \frac{\mathbf{p}^2}{2m} + \frac{1}{2}m(\omega_x^2 x^2 + \omega_y^2 y^2) \right) \otimes \hat{I} + \alpha_R(\hat{\sigma}_x p_y - \hat{\sigma}_y p_x) + h_z \hat{\sigma}_z, \quad (6)$$

where  $\mathbf{p} = \{p_x, p_y\}$  and  $\mathbf{r} = \{x, y\}$  are the 2D momentum and coordinate operators,  $\omega_x$  and  $\omega_y$  are the frequencies of the harmonic oscillator trap in the directions  $x$  and  $y$ ,  $\hat{I}$  is the  $2 \times 2$  unit matrix. The spin-orbit coupling term is given in a Rashba-like form [6],  $\alpha_R(p_x \hat{\sigma}_y - p_y \hat{\sigma}_x)$ , where  $\alpha_R$  is the strength of the spin-orbit coupling,  $\hat{\sigma}_x$ ,  $\hat{\sigma}_y$  and  $\hat{\sigma}_z$  are the  $2 \times 2$  Pauli matrices and  $h_z \hat{\sigma}_z$  is the Zeeman term.

The hamiltonian (6) without the Zeeman term commutes with the time reversal operator, which for spin- $\frac{1}{2}$  particles can be written as

$$\hat{T} = i\hat{\sigma}_y K, \quad (7)$$

where  $K$  is the complex conjugation operator [46]. For this system the eigenenergies are two-fold (Kramers) degenerate. For the case of equal frequencies ( $\omega_x = \omega_y$ ) the system is cylindrically symmetric. The deformation of the confining harmonic potential ( $\omega_x \neq \omega_y$ ) breaks the cylindrical rotational invariance. In this case we have a reason to believe that the level repulsion should be rather strong and the Wigner distribution with  $\beta = 4$  could arise. If we add an additional external Zeeman field the time-reversal symmetry is also broken and the distribution with  $\beta = 2$  is suggested.

We emphasize that it is not at all necessary to arrive at one of the distributions in Eqs. (1)-(5). Any combination or totally different results are perhaps more likely. However, given sets of the tunable parameters may produce these standard distributions, and thereby provide hamiltonians corresponding to pure regular or chaotic motion. We shall therefore perform the appropriate statistical analysis of the energy spectra in order to understand these features better.

The eigenstates of the hamiltonian (6) were previously calculated using the exact diagonalisation method [23], which we adopt for the present paper. We expand the eigenstates on a basis of harmonic oscillator wave functions. The oscillator potential is deformed and clearly

suggesting a corresponding set of basis functions. However, the spin-orbit coupling is then far from diagonal and relatively high-lying states can be expected necessary. We still choose the deformed Cartesian oscillator basis of the oscillator trap. The energy units, or equivalently the spatial extension, may be very different for the  $x$  and  $y$ -directions. To account roughly for the deformation effect in the basis, we include all states up to the same maximum energy,  $E_{max} \approx N_x \omega_x \approx N_y \omega_y$ , where  $N_x$  and  $N_y$  are the largest directional Cartesian quantum numbers.

In the statistical analyses we have to choose the energy window of eigenvalues such that the number of levels are neither too small nor too large. Too few levels do not allow proper statistics and too many emphasize the basis properties instead of the interactions in the hamiltonian. To be clear about this, a large number of levels may all be found numerically as precise eigenvalues, but inclusion of all such high-energy solutions in an analysis would not provide useful dynamical information about the behavior of the system. The most appropriate energy interval depends on the interactions. Our choice of moderate spin-orbit strengths allow a reasonable guess of energy window independent of choice of the controllable parameters. In this paper we analyse usually the lowest 150 doubly degenerate levels, while they are obtained by any basis with more than 700 correspondingly degenerate states. The average maximum quantum number in each direction is then for 700 states about 26. Then all states in the analyses are fully converged.

The calculated energy spectra depend on the three parameters: the spin-orbit coupling strength,  $\alpha_R$ , the deformation,  $\gamma = \omega_x/\omega_y$ , of the trap, and the Zeeman strength,  $h_z$ . Since essentially all symmetries are broken for general values of the deformation, we can expect the repulsive behavior between the energy levels seen as avoided crossings. This might be a signature of chaos in the system, and the Zeeman term might possibly be used to move between the quadratic and quartic Wigner distributions.

### C. Statistical treatment

The set of eigenvalues,  $\{\varepsilon_i\}$ , derived from the Schrödinger equation with the hamiltonian (6) now has to be analysed. First, we note that for the analysis of nearest neighbor distributions systematic degeneracies can be removed, since they only add points of zero spacing. For the present case, the system with  $h_z = 0$  obeys time-reversal symmetry, and in that case all levels are doubly degenerate where only one set has to be treated. Second, the analysis in terms of dimensionless distributions requires removal of the scale carrying the unit of energy. In addition, it is also necessary to even out the average scales of the spacings between the nearest energy levels arising from the different density of the energy spectrum.

We introduce the staircase function:

$$\sigma(\varepsilon) = \frac{1}{N} \int_{-\infty}^{\varepsilon} \sum_{i=1}^N \delta(\varepsilon' - \varepsilon_i) d\varepsilon', \quad (8)$$

where  $\varepsilon$  is an energy value,  $N$  is the number of levels included in the analysis, and  $\delta$  is the Dirac delta function. This function calculates the number of available levels below a given energy and carries the properties of the single-particle level spectrum used in our statistical analyses.

To smooth out  $\sigma(\varepsilon)$  we substitute each delta function by a continuous normalized distribution centered at the same energy. For calculational simplicity we choose normalized Gaussians, hence obtaining

$$\bar{\sigma}_{\Delta}(\varepsilon) = \frac{1}{\Delta\sqrt{\pi}} \frac{1}{N} \int_{-\infty}^{\varepsilon} d\varepsilon' \sum_{i=1}^N e^{-\left(\frac{\varepsilon' - \varepsilon_i}{\Delta}\right)^2} \times \left( \frac{15}{8} - \frac{5}{2} \left( \frac{\varepsilon' - \varepsilon_i}{\Delta} \right)^2 + \frac{1}{2} \left( \frac{\varepsilon' - \varepsilon_i}{\Delta} \right)^4 \right), \quad (9)$$

where the smearing parameter,  $\Delta$ , appears as the width of the Gaussians. The fourth order polynomial guarantees that any initial smooth behavior reproducible by such a polynomial correctly reappears after the smoothing [24]. Different polynomial orders can be chosen but fourth order is sufficient to provide a reasonable stability range in  $\Delta$ , where  $\bar{\sigma}_{\Delta}(\varepsilon)$  in practice is essentially independent of  $\Delta$ .

Finally, to obtain a spectrum with an average level spacing normalized to one, we map the spectrum  $\{\varepsilon_i\}$  onto a new spectrum,  $\{e_i\}$ , defined by

$$e_i = N \bar{\sigma}_{\Delta}(\varepsilon_i), \quad (10)$$

for  $i = 1, \dots, N$ . This procedure is usually called *unfolding of the spectrum* [39]. The statistical analysis are now applied on the new scale-independent and dimensionless spectrum,  $\{e_i\}$ .

It is not surprising that for reasonable statistical analysis the number of levels  $N$  should be "big enough". The size of it is of course always specific to a problem at hand. The rule of thumb is to make sure that the levels are more or less evenly distributed even before the unfolding of the spectrum. In that case the unfolding works the best and the statistical properties of the spectrum are the most evident.

## III. NUMERICAL RESULTS

To obtain the energy spectra we use the exact diagonalization method described in Ref. [23]. We vary both the strengths,  $h_z$  and  $\alpha_R$ , of the Zeeman and spin-orbit coupling terms, and the deformation of the trap expressed as the ratio of frequencies,  $\gamma = \omega_x/\omega_y$ , in  $x$  and  $y$  directions. We focus mostly on the spin-orbit strength which

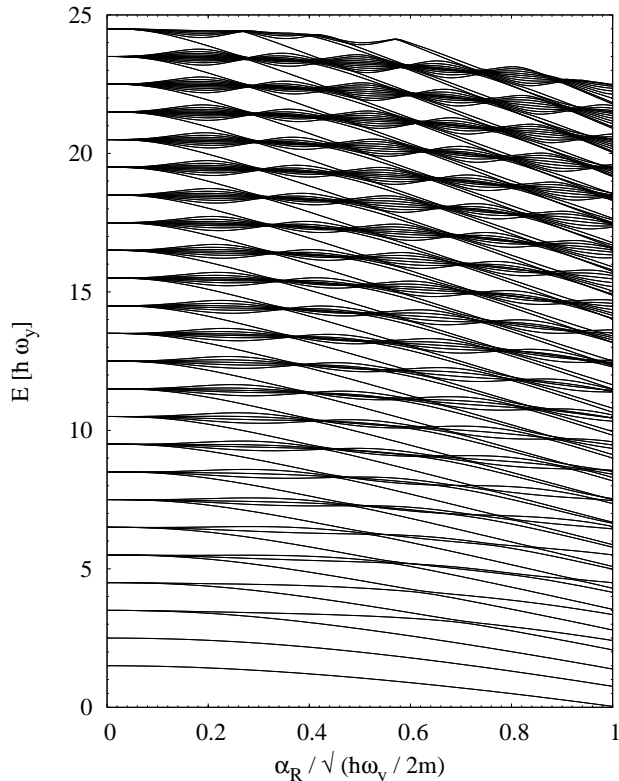


FIG. 2: The energy levels of a spin-orbit coupled particle with  $h_z = 0$  in a deformed harmonic trap as a function of spin-orbit coupling strength. The deformation is  $\gamma = 2$ . The levels from 0 to 300 are shown (notice that levels are two-fold degenerate).

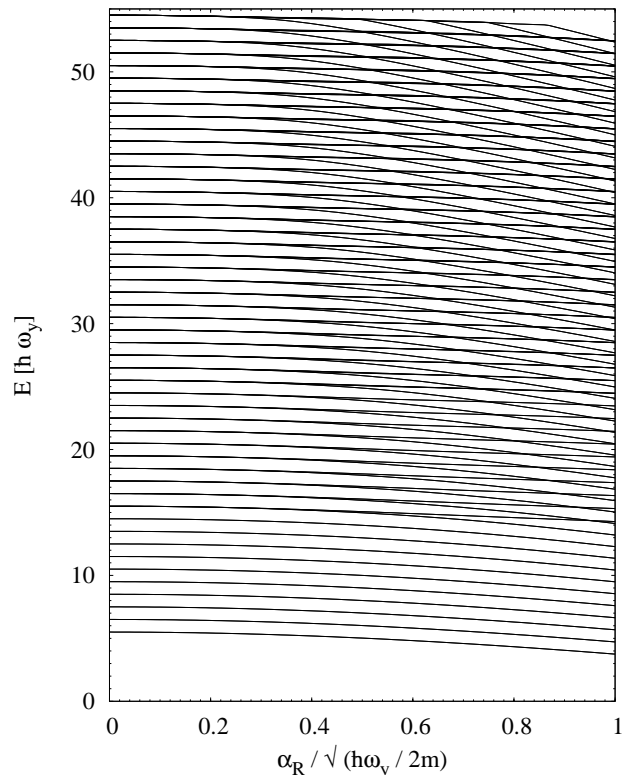


FIG. 3: The energy levels of a spin-orbit coupled particle with  $h_z = 0$  in a deformed harmonic trap as a function of spin-orbit coupling strength. The deformation is  $\gamma = 10$ . The levels from 0 to 300 are shown (notice that levels are two-fold degenerate).

therefore is used as the parameter in all figures. We confine ourselves to strengths varying from zero to the natural value in oscillator units,  $\sqrt{\hbar\omega_y}/(2m)$ . For much larger values the spin-orbit would be dominating and the Landau-like levels would appear. We want to investigate the interplay between the deformed oscillator trap and the spin-orbit coupling. Therefore we choose these terms of comparable size.

The number of levels per unit energy increases with energy and the lowest are usually less significant due to their relative small numbers. However, they may also exhibit a completely different structure as exemplified by a large deformation where 1D structure appears at the bottom of the spectrum and 2D is restored at energies higher than  $\hbar$  times the perpendicular frequency. This dependence on energy window is important. We select one intermediate energy cutoff which is characteristic for the results. At the end of this section we discuss briefly the level distributions for different windows.

### A. Implications of symmetries

We first must identify possible symmetries, remove systematic degeneracies, separate eigenvalues and eigenstates in sets corresponding to conserved quantum numbers, and treat each decoupled set independently. The 2D oscillator alone is known to have a series of degeneracies for integer values of  $\gamma$ , and the smallest integers have largest degeneracy. These real crossings (not avoided) are present because the uncoupled levels are defined by the conserved oscillator quanta in the two directions. The degeneracies are connected to the classical orbits defined as closed paths by successive reflection on the potential walls [47].

Close to these deformations with special oscillator degeneracy there must be many close-lying levels due to the small degeneracy breaking. In addition the other nearest neighbors, above and below each of these near-degenerate levels, are much further apart. Thus, we can expect an unfolded distribution with peaks at small distance and a peaked distribution at distances larger than the average from the spectral theory of random matrices.

Addition of the spin-orbit coupling lifts the oscillator

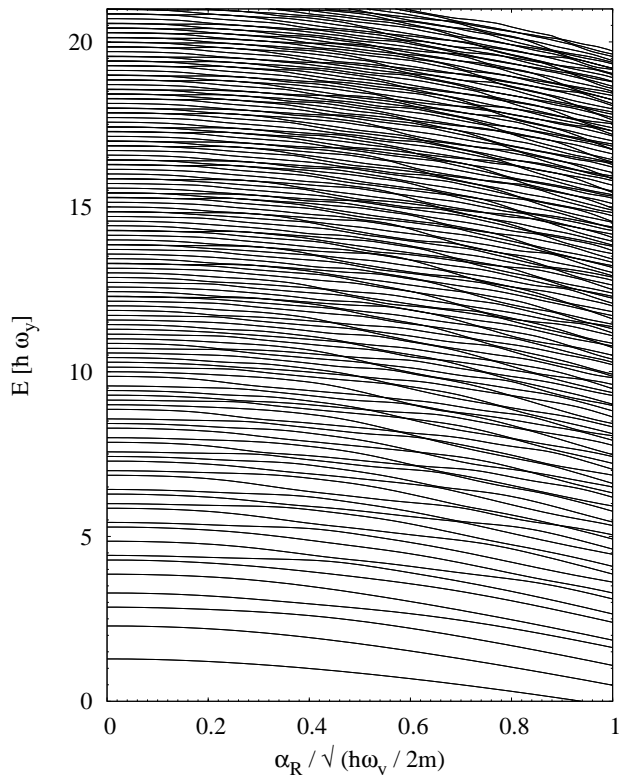


FIG. 4: The energy levels of a spin-orbit coupled particle with  $h_z = 0$  in a deformed harmonic trap as a function of spin-orbit coupling strength. The deformation is  $\gamma = 1.57$  (left). The levels from 0 to 300 are shown (notice that levels are two-fold degenerate).

degeneracy and destroys the related symmetries. Level couplings are now present, conserved quantum numbers essentially disappeared, and the remaining time-reversal symmetry for  $h_z = 0$  only produces doubly degenerate levels. The energy levels are now prohibited to cross and the spectrum appears to have a "band structure".

The origin of these "bands" is intuitively quite clear: the spin-orbit coupling lifts the oscillator degeneracy in a way not unlike, for instance the Zeeman splitting of levels. The avoiding crossing, on the other hand, also controls the behavior of levels and leads to the opening and closing of the "gaps" and, thus, to the "band structure".

The deformation affects this structure. The deformed oscillator levels are shifted compared to non-deformed ones and the degeneracies might be lifted. However, for integer frequency ratios, energy levels (except for the lowest ones) are still degenerate, because in this case they are shifted by an integer number of oscillator quanta. This means that the "band structure" does not disappear, but still exists in the spectrum in the presence of the spin-orbit coupling. This is illustrated in Fig. 2 for the frequency ratio of  $\gamma = 2$ .

An extreme case of large frequency ratio of  $\gamma = 10$  is

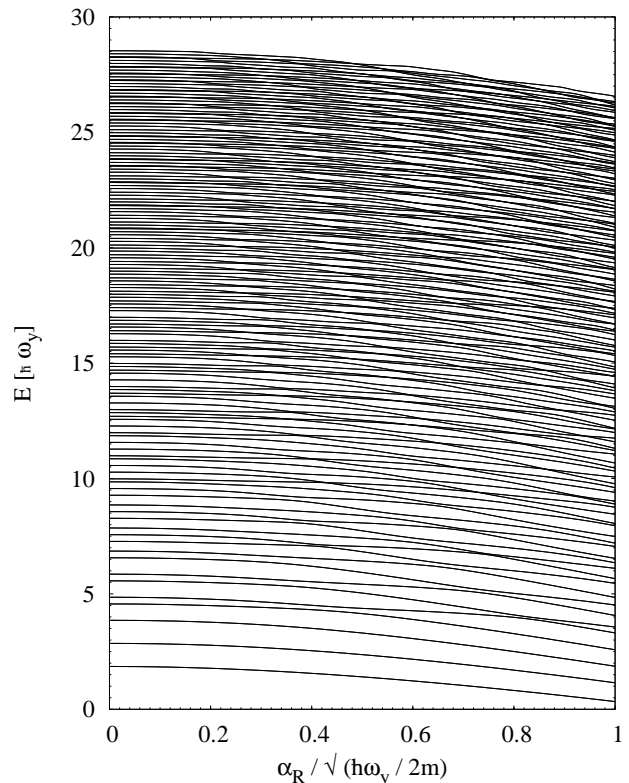


FIG. 5: The energy levels of a spin-orbit coupled particle with  $h_z = 0$  in a deformed harmonic trap as a function of spin-orbit coupling strength. The deformation is  $\gamma = 2.71$ . The levels from 0 to 300 are shown (notice that levels are two-fold degenerate).

shown in Fig. 3. The same pattern of degeneracy restoring as for  $\gamma = 2$  is seen but now appearing only for much larger strengths,  $\alpha_R$ , and at higher energies. The 1D limit is efficiently established for the lowest levels corresponding to energies where the excitations in  $x$ -direction are almost forbidden. We then conclude that destruction of symmetries or lifting degeneracies by using non-integer frequency ratios seems to be as effective both with and without spin-orbit coupling, although additional interaction between levels must tend to randomize better.

The energy levels should be much more evenly distributed for non-integer frequency ratios where oscillator degeneracies are much more rare. In Figs. 4 and 5 we show spectra for  $\gamma = 1.57$  and  $\gamma = 2.71$  where the latter is rather far from any ratio of very small integers, the closest are  $8/3$  and  $11/4$ . The white regions ("gaps") are still clearly visible. However, the structures are now much weaker and apparently almost vanishing for the highest energies in the spectrum.

So far we omitted the Zeeman field which may introduce new features since it breaks the Kramers degeneracy. In Figs. 6 and 7 we show spectra with finite Zeeman field and the broken rotational symmetry. The number of levels now doubled due to breaking the time-reversal

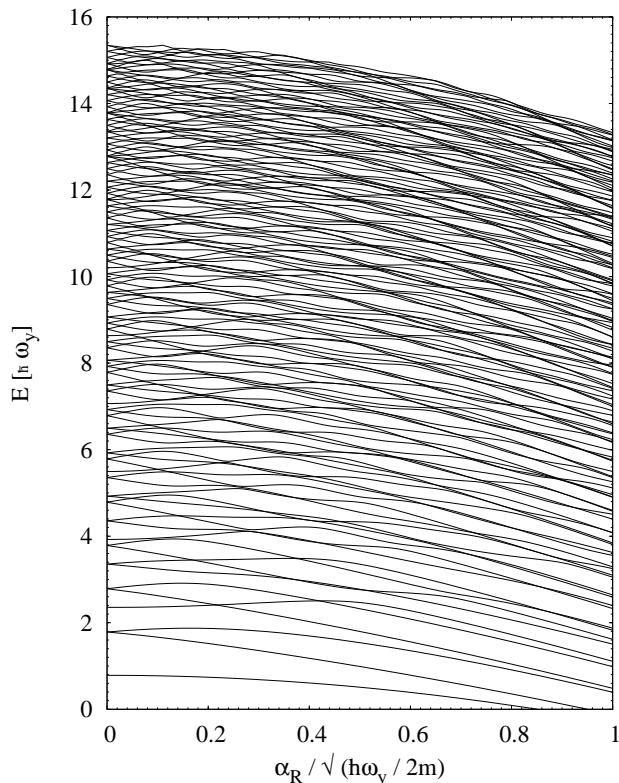


FIG. 6: The energy levels of a spin-orbit coupled particle in a deformed harmonic trap as a function of spin-orbit coupling strength. The deformation  $\gamma = 1.57$ . The Zeeman strength is  $h_z = 0.5\hbar\omega_y$ . The levels from 0 to 150 are shown.

symmetry. The denser spectra have now only avoided level crossings even though several levels appear to be very close-lying. In any case the degree of level repulsion cannot be read directly off from these plots.

The repulsion between energy levels is always present in some limited regions of energy for corresponding deformations and interaction strengths. From the presented level spectra it is clear that a given hamiltonian with both finite deformation and spin-orbit interaction only lead to occasional avoided crossing regions in rather small energy windows.

A special type of symmetry is related to the spin-orbit coupling via the balance of the two terms,  $\hat{\sigma}_y p_x$  and  $\hat{\sigma}_x p_y$ . Varying their relative strengths continuously from  $-1$  to  $1$  change the spectra substantially. The symmetry between the  $x$  and  $y$  directions implies that the Rashba ( $-1$ ) and Dresselhaus ( $1$ ) spin-orbit couplings produce identical spectra. When one of the spin-terms is removed the hamiltonian decouples into two  $1D$  contributions, where each roughly speaking is a shifted oscillator. Thus, such parameter variations change from Rashba coupling to an effective  $1D$  hamiltonian. The intermediate situation when the spin-orbit coupling strengths are not equal is usually referred as the anisotropic spin-orbit coupling in a spherical  $2D$  trap. The hamiltonian is then equiva-

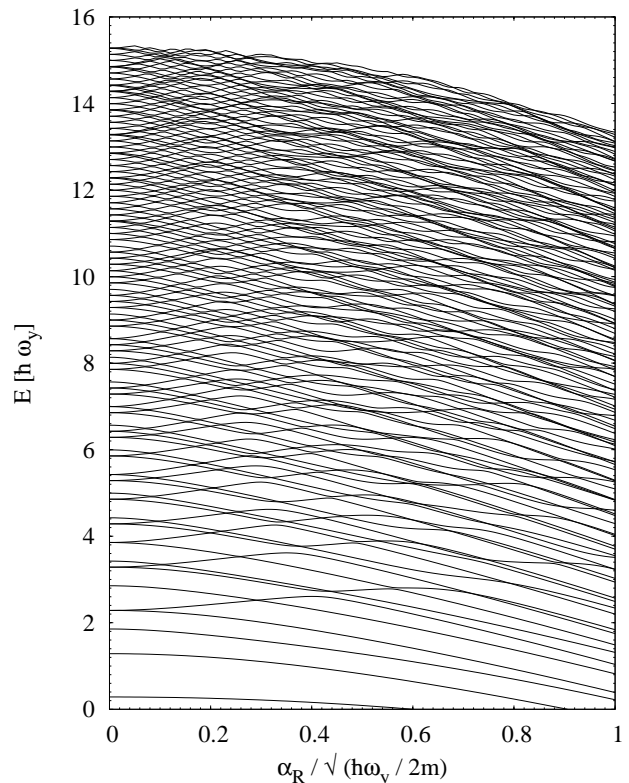


FIG. 7: The energy levels of a spin-orbit coupled particle in a deformed harmonic trap as a function of spin-orbit coupling strength. The deformation  $\gamma = 1.57$ . The Zeeman strength is  $h_z = \hbar\omega_y$ . The levels from 0 to 150 are shown.

lent to that of the Jahn-Teller model [48]. This model and its relation to the irregular dynamics have been studied in Refs. [49–52]. While we will not consider anisotropic spin-orbit terms in this paper we compare and contrast the present study to previous work on the Jahn-Teller model.

## B. Nearest neighbor distributions

The distributions are the first step to pin-point an underlying regular or irregular motion. To determine whether a system is quantum chaotic or not typically requires an analysis of the equivalent classical problem [39, 40]. Such a full analysis for the system in an isotropic ( $\omega_x = \omega_y$ ) trap with anisotropic spin-orbit coupling ( $\hat{V}_{SOC} = \alpha_1 \hat{\sigma}_x p_y + \alpha_2 \hat{\sigma}_y p_x$ , with  $\alpha_1 \neq \alpha_2$ ) was recently published in Ref. [53]. The analysis presented in that paper can be carried out for our system as well and we assume that the correspondence between classical and quantum chaotic behaviour holds in our case as well. A very interesting recent study of quantum billiard with spin-orbit coupling [54] provides further evidence that chaos will arise for spin-orbit coupled systems in

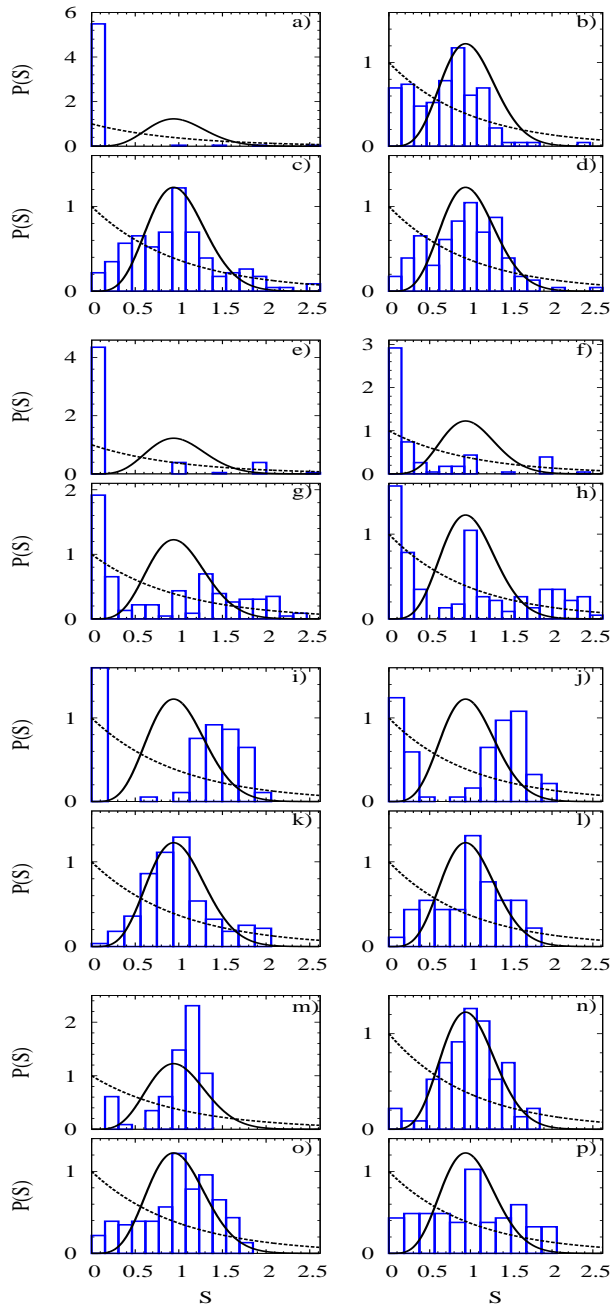


FIG. 8: The nearest neighbor level spacing distribution for different sets of parameters values. For deformation  $\frac{\omega_x}{\omega_y} = 2$ : a)  $\alpha_R = 0$ , b)  $\alpha_R = 0.3$ , c)  $\alpha_R = 0.5$ , and d)  $\alpha_R = 0.7$ . For deformation  $\frac{\omega_x}{\omega_y} = 10$ : e)  $\alpha_R = 0$ , f)  $\alpha_R = 0.3$ , g)  $\alpha_R = 0.5$ , and h)  $\alpha_R = 0.7$ . For deformation  $\frac{\omega_x}{\omega_y} = 1.57$ : i)  $\alpha_R = 0$ , j)  $\alpha_R = 0.3$ , k)  $\alpha_R = 0.5$ , and l)  $\alpha_R = 0.7$ . For deformation  $\frac{\omega_x}{\omega_y} = 2.71$ : m)  $\alpha_R = 0$ , n)  $\alpha_R = 0.22$ , o)  $\alpha_R = 0.3$ , and p)  $\alpha_R = 0.5$ . We use units  $\sqrt{\frac{\hbar\omega_y}{2m}}$  for the spin-orbit coupling parameter  $\alpha_R$ . The external magnetic field  $h_z = 0$ . The distributions are compared to the Poisson (dashed line) and Wigner (4) (solid line) distributions.

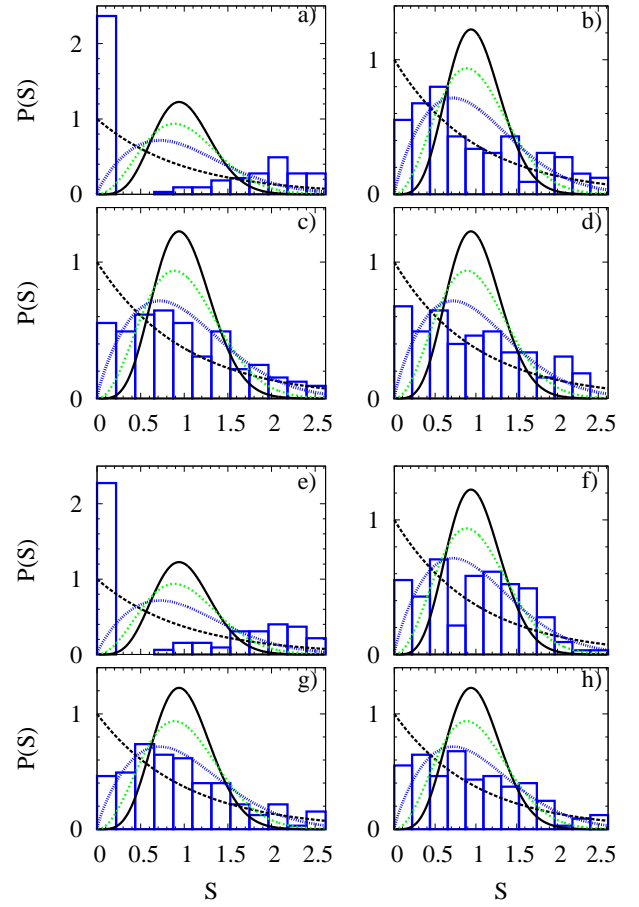


FIG. 9: The nearest neighbor level spacing distribution for different values of spin-orbit coupling parameter,  $\alpha_R$ , in units of  $\sqrt{\frac{\hbar\omega_y}{2m}}$ : a) and e)  $\alpha_R = 0$ , b) and f)  $\alpha_R = 0.3$ , c) and g)  $\alpha_R = 0.5$ , d) and h)  $\alpha_R = 0.7$ . The cases from a) to d) correspond to the Zeeman strength  $h_z = \hbar\omega_y/2$  and the cases e) to h) correspond to  $h_z = \hbar\omega_y$ . The harmonic trap frequencies ratio  $\frac{\omega_x}{\omega_y} = 1.57$ . The distributions are compared to the Poisson (dashed line), Brody (solid blue line) (5), quadratic Wigner (solid green line) (3) distributions, and quartic Wigner (solid black line) (4) distributions. The Brody parameter is  $\kappa = 0.4$ .

two dimensions.

Within the context of the Jahn-Teller model, the level distributions statistics have been considered in previous works [50–52]. The Hamiltonian in those papers can be mapped to isotropic and anisotropic spin-orbit couplings in a spherical 2D harmonic oscillator in our setup. Furthermore, a Jahn-Teller equivalent of a deformed oscillator discussed in Ref. [49] was shown to have signatures of chaos in the quantum dynamics although no level distributions were considered. In Ref. [50] it was suggested that anharmonic (oscillator) terms could be used to drive the level distribution from Poisson (1) to Wigner (2) and that such anharmonicity could be a requirement for chaotic behaviour. However, subsequent studies in Refs. [51, 52] have found substantial deviations from the

Poisson (1) distribution without including anharmonicity. In Ref. [51] these deviations are analyzed using distributions different from Wigner (2). The results presented below also go beyond the Poisson (1) and Wigner (2) distributions. By using a combination of Rashba spin-orbit coupling, and deformed trap and a Zeeman field we find parameter regimes where the Wigner (4) and the Brody (5) distributions may be realized. While the Brody distribution has been discussed in the context of the Jahn-Teller model previously [51], the fourth order Wigner (4) was not observed as far as we can tell.

Apart from the extreme limits of huge deformation or huge spin-orbit strengths, we expect the spectra of a 2D deformed oscillator to have different properties due to the breaking of the cylindrical symmetry seen in the non-deformed case. The oscillator degeneracies are varying very strongly from spherical to well deformed. For a small number of rational frequency ratios the degeneracies are largest, but for irrational frequency ratios the degeneracies have effectively completely disappeared. This is directly related to properties of the level spectra and therefore decisive for underlying regular or chaotic motion.

We shall first only examine the statistical behavior as a function of deformation and spin-orbit strength with  $h_z = 0$ . The analysis provides nearest neighbor distributions which we shall present as histograms derived from the unfolded spectrum. As references we compare the results with the extremes of the Poisson and Wigner distributions Eqs. (1) and (4). We avoid the most symmetric case of the spherical oscillator where the regular structure and large degeneracy initially prohibits a meaningful statistical analysis. Still for a frequency ratio of 2 without spin-orbit, see Fig. 8a, the level distribution is trivial with many nearest neighbors of either zero distance or reflecting the regularity of the oscillator degeneracy. These features change as the spin-orbit coupling is switched on. For all finite strengths shown in Fig. 8 we find structures resulting from incoherent and sizewise comparable contributions of the Poisson,  $P_P$ , and Wigner,  $P_{W4}$ , distributions.

The other special case of deformation is shown in Fig. 8(e-h) for a frequency ratio of 10. The lowest part of the spectrum reflects the regularity of a 1D oscillator in Fig. 3, whereas the 2D behavior emerges only at higher energies. For larger strengths and higher energies the spectral pattern resembles a condensed version of the structure for frequency ratio 2. The nearest neighbor distribution still reveals a large peak at small level distance and irregular contributions for larger level distances.

The lack of symmetries for non-integer frequency ratios leads to the distributions shown in Figs. 8(i-p). We can see that in both cases the Wigner distribution,  $P_{W4}$ , is realized for particular values of the spin-orbit coupling strength:  $\alpha_R/\sqrt{\frac{\hbar\omega_y}{2m}} = 0.5$  for  $\gamma = 1.57$ , Fig. 8k, and  $\alpha_R/\sqrt{\frac{\hbar\omega_y}{2m}} = 0.21$  for  $\gamma = 2.71$ , Fig. 8n. It implies that in the vicinity of these values our system is likely to be

in the quantum chaotic regime.

Away from oscillator isotropy the level statistics is quite different. For small spin-orbit parameter the statistical behavior is defined by the initial oscillator spectrum. If the higher oscillator levels are "almost degenerate" in the sense that the difference between levels much is much smaller than  $\hbar\omega_y$  even after the deformation, then it will appear on the histogram as a strong peak near the point  $S = 0$ , see Fig. 8i. In Fig. 8m one sees a different picture: there is no peak at  $S = 0$  due to more evenly distributed oscillator eigenlevels.

Combining spin-orbit coupling and deformation introduce a distribution altogether different from either spin-orbit or deformation separately. Absence of the quantum mechanical integrals of motion leads to series of energy levels with avoided crossings. The spectra can be far from the ordered oscillator structures. The regions with few levels are smaller and much less frequent. The pattern seen in Figs. 2-5 are level structures where low density regions move depending on energy and spin-orbit strength. The levels for one strength are therefore much more uniformly distributed. Finite spin-orbit and deformation do not in general allow symmetries or degeneracies, although a number of individual almost crossing levels appear in level diagrams. However, they are few and in fact avoided crossings. The NNS distributions are therefore more likely to follow one of the Wigner distributions.

In Fig. 9 we show the NNS distribution of levels in the presence of the Zeeman term. We consider the same cases of the trap deformation and the spin-orbit coupling strength as in Fig. 8. The Kramers degeneracy is lifted by the Zeeman term and its strength,  $h_z$ , is another parameter varying the NNS distribution. We see that for non-zero values of the spin-orbit coupling strength the histograms are reproduced very well by the Brody distribution with a value of the Brody parameter of  $\kappa = 0.4$ . This is somewhat surprising, since after lifting the Kramers degeneracy one would intuitively expect better agreement with the second (not first) power Wigner distribution (3) [39].

We have so far only shown distributions for 150 (double or single) degenerate levels. The most interesting variation is to see whether the Wigner distribution depends on the energy window. The results are shown in Fig. 10 for two distributions corresponding to irregular dynamic motion with 150 levels. The systematic behavior is that an intermediate number of levels leave the Wigner distribution essentially unchanged. Many more levels, where the effect of the interaction fade away, increases the probability at small distances and the distribution would eventually approach a Poisson distribution reflecting very regular motion. Fewer of the low-lying levels must eventually describe, perhaps statistically insignificantly, the properties of the very small excitations. By reduction of window size these Wigner-like distributions can then move in any direction.

We also changed window size away from 150 levels for

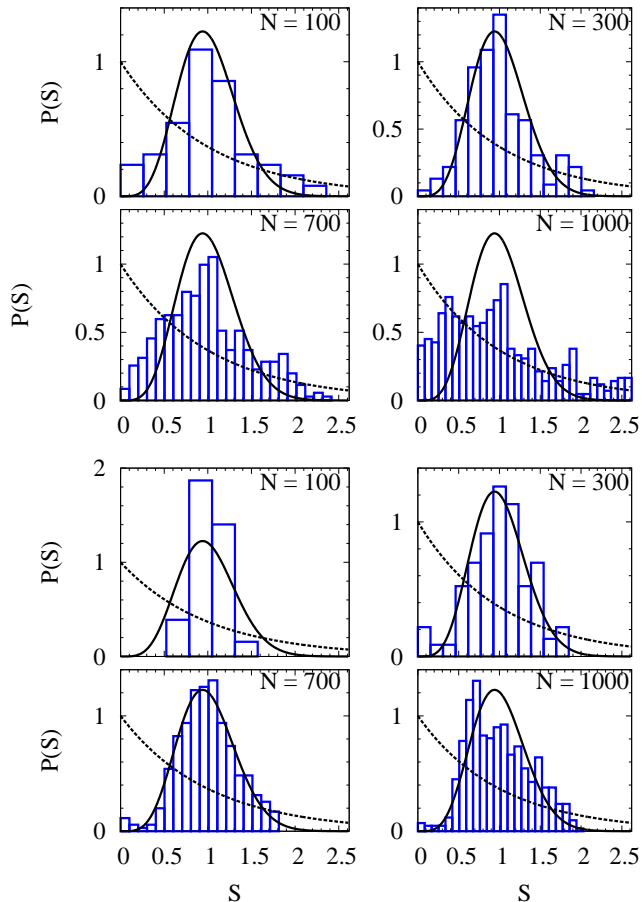


FIG. 10: The nearest neighbor level spacing distribution for different energy windows determined by the number of levels included in the analysis. The top four figures are for  $\frac{\omega_x}{\omega_y} = 1.57$  and  $\alpha_R/\sqrt{\frac{\hbar\omega_y}{2m}} = 0.5$ . The bottom four figures are for  $\frac{\omega_x}{\omega_y} = 2.71$  and  $\alpha_R/\sqrt{\frac{\hbar\omega_y}{2m}} = 0.21$ . The number of the lowest energy levels used in the analysis is given in the figures. The distributions are compared to the Poisson (dashed line) and Wigner (4) (solid line) distributions.

cases where the Wigner distribution is far from being followed. The results are systematically that Wigner-like distributions do not appear when absent for the intermediate number of levels in the energy window. Thus, we conclude that the 150 levels used throughout the present series of analyses is a characteristic number of levels well suited to search for possible irregular motion.

#### IV. CONCLUSIONS

In this article we discuss the statistical properties of the spectrum of energy eigenvalues for a two-dimensional one-body hamiltonian with Rashba spin-orbit and Zeeman terms and a deformed harmonic oscillator. We summarized some of the possible statistical distributions that

we may expect for the nearest neighbors energy separation. These schematic limiting distributions emerge as results from random matrix eigenvalues with different symmetries. In particular we have regular integrable motion, and irregular chaotic motion with and without time-reversal symmetry or Kramers degeneracy.

We calculate spectra as function of three parameters, that is deformation as frequency ratios, and spin-orbit and Zeeman strengths. To investigate the statistics we use the so-called unfolding procedure to remove the overall energy scale along with unimportant obscuring average properties. The results exhibit a huge variety of the nearest neighbor distributions. Several parameter limits produce simple and well-known spectra especially obvious when one of the three terms in the hamiltonian is overwhelmingly dominating. The same conclusion about emerging stability holds when the two spin-orbit coupling terms are extremely unevenly weighted. All these cases are analytically solvable, i.e. either a cylindrical oscillator, a spin-orbit term or a Zeemann field without the other two. In addition, a large deformation is equivalent to a one-dimensional system with very simple oscillator-like properties for all values of spin-orbit and Zeeman terms. These limits are uninteresting for statistical properties, and intermediate parameter values are necessary to get sufficiently different couplings.

We first search for structure without Zeeman field. Small integral frequency ratios are too degenerate to provide irregular solutions. For most parameter choices the nearest neighbor distribution is far from any of the schematic random matrix results. Systematic resemblance is difficult to find and linear combinations of Poisson and Wigner distributions are probably the closest similarity. However, we do find indications of chaotic motion with a fourth-power level-repulsion term for some irrational frequency ratios and specific spin-orbit strengths. Including a finite Zeeman field breaks time-reversal symmetry and is therefore potentially able to lead to a different chaotic motion corresponding to a second-power level-repulsion term. However, we see a quite different behavior: the histograms for finite values of the spin-orbit coupling are described very well by an intermediate Brody distribution.

Our numerical results suggest that a combination of trap deformation, spin-orbit coupling strength and Zeeman field provides a suitable tool to manipulate the spectrum. Some parameters give the Wigner nearest neighbor distribution which is used as a signature of a quantum chaotic system. The spin-orbit coupling appear as a valuable tool to investigate regimes of such irregular motion. This is within practical reach in present cold atomic gas experiments where a highly tunable single-particle spin-orbit coupling is already available. Thus the perspective is that the transition between regular and chaotic motion can be systematically investigated by varying the spin-orbit strength for given deformations. The Zeeman field can also be used to change the distribution towards another Wigner distribution corresponding to less level

repulsion.

These results can also be looked at from the perspective of a non-interacting system of  $N$  fermions. In this case particles occupy  $N$  energy levels so that the Fermi energy would be equal to the  $(N/2)$ 'th energy level (due to the Kramers degeneracy). The dynamics of such systems will be defined by the statistical properties of the spectrum around the Fermi energy. The requirement is tunability of the deformation and subsequent variation of the spin-orbit strength to move from regular to quantum chaotic systems. The experimental capabilities and interest in use of cold atoms with Rashba-like spin-orbit interactions should make fermionic  $N$ -body systems re-

alizable in the near future. An interesting question is the role of interactions. Within a mean-field Hartree-Fock method using repulsive zero-range interactions, the structure of the single-particle Hartree-Fock energy levels stays qualitatively the same as the non-interacting spectrum [55]. However, the number of particles and the strength of interaction are the additional parameters to control the statistical properties of the spectrum. Thus, a more in-depth analysis of the interacting system is an interesting direction for future work.

We thank Jonas Larson for valuable discussions. This work was supported by the Danish Council for Independent Research - Natural Sciences.

- 
- [1] Ketterle W and Zwierlein M W 2008 *Nuovo Cimento Rivista Serie* **31** 247
- [2] Bloch I, Dalibard J and Zwerger W 2008 *Rev. Mod. Phys.* **80** 885
- [3] Esslinger T 2010 *Ann. Rev. Cond. Mat. Phys.* **1** 129
- [4] Cirac J I and Zoller P 2012 *Nature Phys.* **8** 264
- [5] Dalibard J, Gerbier F, Juzeliūnas G and Öhberg P 2011 *Rev. Mod. Phys.* **83** 1523
- [6] Bychkov Yu A and Rashba E I 1984 *J. Phys. C: Solid State Phys.* **17** 6039
- [7] Anderson B P, Juzeliūnas G, Spielman I B and Galitski V M 2012 *Phys. Rev. Lett.* **108** 235301
- [8] Goldman N, Juzeliūnas G, Öhberg P, Spielman I B 2013 *Preprint* arXiv:1308.6533
- [9] Lin Y-J *et al* 2009 *Phys. Rev. Lett.* **102** 130401
- [10] Lin Y-J, Compton R L, Jiménez-García K, Porto J V and Spielman I B 2009 *Nature* **462** 628
- [11] Lin Y-J, Jiménez-García K and Spielman I B 2009 *Nature* **471** 83
- [12] Aidelsburger A *et al* 2011 *Phys. Rev. Lett.* **107** 255301
- [13] Zhang J-Y *et al* 2012 *Phys. Rev. Lett.* **109** 115301
- [14] Wang P *et al* 2012 *Phys. Rev. Lett.* **109** 095301
- [15] Cheuk L *et al* 2012 *Phys. Rev. Lett.* **109** 095302
- [16] Ghosh S K, Vyasankere J P and Shenoy V B 2011 *Phys. Rev. A* **84** 053629
- [17] Sinha S, Nath R and Santos L 2011 *Phys. Rev. Lett.* **107** 270401
- [18] Hu H, Ramachandran B, Pu H and Liu X-J 2012 *Phys. Rev. Lett.* **108** 010402
- [19] Ramachandran B, *et al* 2012 *Phys. Rev. A* **85** 023606
- [20] Stanescu T D, Zhang C, and Galitski V 2007 *Phys. Rev. Lett.* **99** 110403
- [21] Stanescu T D, Anderson B, and Galitski V 2008 *Phys. Rev. A* **78** 023616
- [22] Dresselhaus G, 1955 *Phys. Rev.* **100**
- [23] Marchukov O V *et al* 2013 *J. Phys. B: At. Mol. Opt. Phys.* **46** 134012
- [24] Brack M *et al* 1972 *Rev. Mod. Phys.* **44** 320
- [25] Berry M V and Tabor M 1977 *Proc. R. Soc. Lond. A* **356** 375
- [26] Bohigas O, Giannoni M J and Schmit C 1984, *Phys. Rev. Lett.* **52** 1
- [27] Heusler S, Müller S, Atland A, Braun P and Haake F 2007 *Phys. Rev. Lett.* **98** 044103
- [28] Graham R, Schlautmann M and Zoller P 1992 *Phys. Rev. A* **45** R19(R)
- [29] Moore, F L, Robinson J C, Bharucha C, Williams P E and Raizen M G 1994 *Phys. Rev. Lett.* **73** 2974
- [30] Moore, F L, Robinson J C, Bharucha C F, Sundaram B and Raizen M G 1995 *Phys. Rev. Lett.* **75** 4598
- [31] d'Arcy M B, Summy G S, Fishman S and Guarneri I 2004 *Phys. Scr.* **69** C25
- [32] Klappauf B G, Oskay W H, Steck D A and Raizen M G 1999 *Physica D* **131** 78
- [33] Steck D A, Oskay W H and Raizen M G 2001 *Science* **293** 274
- [34] Stone C, Ait-El-Aoud Y, Yurovsky V A and Olshanii M 2010 *New J. Phys.* **12** 055022
- [35] Graß T, Juliá-Díaz B, Kuś M and Lewenstein M 2013 *Phys. Rev. Lett.* **111** 090404
- [36] Mumford J, Larson J, and O'Dell D H J 2014 *Phys. Rev. A* **89** 023620
- [37] Frisch A *et al* 2014 *Nature* **507** 475
- [38] Guhr T, Müller-Groeling A and Weidenmüller H A 1998 *Phys. Rep.* **299** 189
- [39] Haake F *Quantum Signatures of Chaos* 2001 Springer-Verlag
- [40] Reichl L E *The Transition to Chaos: In Conservative Classical Systems: Quantum Manifestation* 2nd edition 1992 Springer-Verlag
- [41] Mehta M L *Random Matrices* 3rd edition 2004 Elsevier
- [42] Kravtsov V E *Random matrix theory: Wigner-Dyson statistics and beyond. (Lecture notes of a course given at SISSA (Trieste, Italy))* 2012 arXiv:0911.0639
- [43] Brody T A, Flores J, French J B, Mello P A, Pandey A and Wong S S M 1981 *Rev. Mod. Phys.* **53**, 3
- [44] Santos L F and Rigol M 2010 *Phys. Rev. E* **81** 036206
- [45] Sakhr J and Nieminen J M 2005 *Phys. Rev. E* **72** 045204
- [46] Sakurai J J *Modern Quantum Mechanics* 1994 Addison-Wesley Publishing Company
- [47] Brack M and Bhaduri R K *Semiclassical Physics* 1997 Addison-Wesley Publishing Company, Inc.
- [48] Larson J, Sjöqvist E 2009 *Phys. Rev. A* **79** 043627
- [49] Markiewicz R S, 2001 *Phys. Rev. E* **64** 026216
- [50] Yamasaki H, Natsume Y, Terai A and Nakamura K, 2003 *Phys. Rev. E* **68** 046201
- [51] Majerníková E, Shrypko S, 2006 *Phys. Rev. E* **73** 057202
- [52] Majerníková E, Shrypko S, 2006 *Phys. Rev. E* **73** 066215
- [53] Larson J, Anderson B M and Altland A 2013 *Phys. Rev. A* **87** 013624

[54] Khomitsky D V, Malyshev A I, Sherman E Ya and Di  
Ventra M 2013 *Phys. Rev. B* **88** 195407

[55] Marchukov O V *et al* 2014 *Few-Body Syst.* **55** 1045